Journal of Molecular Structure 1049 (2013) 326–335

Contents lists available at SciVerse ScienceDirect

Journal of Molecular Structure

journal homepage: www.elsevier.com/locate/molstruc

Synthesis, spectral, antitumor and antimicrobial studies on Cu(II) complexes of purine and triazole Schiff base derivatives

Said Amer, Nadia El-Wakiel *, Hoda El-Ghamry

Chemistry Department, Faculty of Science, Tanta University, Tanta, Egypt

HIGHLIGHTS

- A new series of Schiff bases of purine and triazole have been synthesized in addition to their Cu(II) complexes.
- The structures of the prepared compounds have been investigated by different spectroscopic techniques.
- The biological and anti-tumor activities for some complexes have been evaluated.

ARTICLE INFO

Article history:
Received 5 March 2013
Received in revised form 24 June 2013
Accepted 24 June 2013
Available online 2 July 2013

Keywords:
Purine
Triazole
Schiff bases
Cu(II) complexes
Antimicrobial
Antitumor

ABSTRACT

A series of copper (II) complexes of Schiff bases derived from 7*H*-2,6-diaminopurine and 4*H*-3,5-diamino-1,2,4-triazole with 2-pyridinecarbaldehyde, salicylaldehyde, 2,4-dihydroxybenzaldehyde and 2-hydroxy-1-naphthaldehyde have been prepared. The donor atoms and the possible geometry of the complexes were investigated by means of elemental and thermal analyses, molar conductance, magnetic moment, UV–Vis, IR, ESR and mass spectra. The ligands behaved as tetradentate, coordinating through the nitrogen atom of the azomethine group and the nearest nitrogen atom to it or oxygen atom of α-hydroxyl group. The results of simultaneous DTA & TGA analyses of the complexes showed the final degradation product for these complexes is CuO. The spectral studies confirmed a four coordinate environment around the metal ion. The obtained results were supported by 3D molecular modeling of complexes using molecular mechanics (MM+) and semiempirical molecular orbital calculations (PM3). These complexes were also tested for their in vitro antimicrobial activities against some bacterial and fungal strains. Complex 2 was investigated for its cyctotoxic effect against human *breast cancer* (MCF7), *liver carcinoma* (HEPG2) and *colon carcinoma* cell lines (HCT116). This compound exhibited a moderate activity against the tested cell lines with IC_{50} of 10.3, 9.8 and 8.7 μg/ml against MCF7, HCT116 and HEPG2, respectively.

1. Introduction

Nitrogen-containing ligands such as Schiff bases and their metal complexes played an important role in the development of coordination chemistry resulting in an enormous number of publications, ranging from pure synthetic work to physicochemical [1] and biochemically relevant studies of metal complexes [2–6] and found wide range of applications. Other kinds of nitrogen-containing ligands are well-known pyrimidine systems such as the purine bases (constituents of the nucleic acids) and their derivatives. These compounds also are of great importance to chemists as well as to biologists as they have been found in a large variety of naturally occurring compounds and also in clinically useful molecules having diverse biological activities [7–9]. Purine bases modified in the 6-position and their derivatives and analogues possess a wide range of biological properties such as antitubercular, fungicidal, antiallergic, antimicrobial, antitumor, antihistamic as well as myocardium inhibiting agent [10–18]. In last few years the interaction of metal ions with nucleic acids has been very active area of inorganic and structural chemistry [9]. The study of metal coordination with the purines reveals in vitro the mechanism of their coordination with DNA [19]. Also, triazoles and their derivatives represent a very interesting class of compounds because of their wide applications as antifungal [20], antibacterial [21], anticancer [22] and antiviral [23] compounds, therefore Schiff bases containing a triazole moiety and their metal complexes are expected to be bioactive compounds [24–26].

It has long been known that metal ions involved in biological processes of life and have been a subject of interest. Among metals, Copper is one of the essential trace elements present in living organisms. It also exhibits considerable biochemical action as a

* Corresponding author.
E-mail address: drnadia6@yahoo.com (N. El-Wakiel).

0022-2860
http://dx.doi.org/10.1016/j.molstruc.2013.06.059

constituent of various exogenous administered compounds in humans. In its latter role it is bound to ligands of various types forming complexes that interact with biomolecules, mainly proteins and nucleic acids. Current interest in Cu complexes is stemming from their potential use as antimicrobial, antiviral, anti-inflammatory and antitumor agents, enzyme inhibitors or chemical nucleases [27,28]. A number of Cu(II) chelate complexes that exhibit cytotoxic activity through cell apoptosis or enzyme inhibition have been reviewed [29]. Such complexes containing bi-Schiff bases as ligands are effective in reducing tumor size, delaying of metastasis and significant increasing survival of the hosts [29].

In attempt to obtain more insight into the bioactivity of nitrogen containing Schiff bases compared with their metal complexes, herein, we have synthesized and characterized a series of purine and 1,2,4-triazole-based Schiff bases and their copper(II) complexes. The in vitro antibacterial, antifungal and anti-tumor activity of some selected compounds has been investigated.

2. Experimental

2.1. Materials and methods

Elemental analyses were performed by the aid of Perkin-Elmer 2400 CHN Elemental analyzer. The metal content of the complexes was determined by atomic absorption spectroscopy using Perkin–Elmer 2380 atomic absorption spectrophotometer after complete decomposition of the complexes in conc. HNO_3 several times. IR spectra were recorded on a Perkin Elmer 1430 instrument (KBr discs) in the 4000–200 cm^{-1} range. Electronic spectra were obtained with a Shimadzu UV–Vis. 240 spectrophotometer using Nujol mull technique. The ESR spectra of powder samples were recorded by means of a Jeol model JES-FE 2XG spectrometer equipped with an E101 microwave bridge. Diphenyl picrylhydrazyl (DPPH) was used as a reference material ($g = 2.0023$). The molar conductance measurements were carried out at room temperature using Hanna 8733 conductivity meter. The room temperature magnetic susceptibility was measured using magnetic susceptibility balance (Johnson Mtthey) 436 Devon Park Drive. The thermal analyses (TGA and DTA) were performed using computerized Shimadzu TG-50 thermal analyzer up to 800 °C at a heating rate 10 °C/min. under nitrogen atmosphere.

2.2. Preparation of ligands L^{1-3}

To a solution of 7H-2,6-diaminopurine (0.001 mol, 0.15 g) in 20 ml ethanol, a solution of 2-pyridinecarbaldehyde (0.002, 0.214 g), 2,4-dihydroxy-1-naphthaldehyde (0.002, 0.138 g) or 2-hydroxy-1-naphthaldehyde (0.002, 0.172 g) in ethanol (20 ml) was added. The resulting mixtures were then refluxed with stirring for 6 h. the products, which separated out on hot, were filtered of, washed with ethanol and dried over anhydrous $CaCl_2$ (Yield: 64–77%).

2.3. Preparation of ligands L^{4-7}

A similar procedures as that described above for synthesis of L^{1-3} were carried out, by mixing an ethanolic solution of 4H-3,5-diamino-1,2,4-triazole (0.001 mol, 0.099 g and 20 ml) and 20 ml ethanolic solution of 2-pyridinecarbaldehyde (0.002, 0.214 g), salicylaldehyde (0.002, 0.122 g), 2,4-dihydroxy-1-naphthaldehyde (0.002, 0.138 g) or 2-hydroxy-1-naphthaldehyde (0.002, 0.172 g). The resulting mixtures were also refluxed with stirring for 6 h. the products, which separated out on hot, were filtered of, washed with ethanol and dried over anhydrous $CaCl_2$ (Yield: 66–84%). The prepared Schiff bases (L^1–L^7) have the following structural formulae (Fig. 1).

2.4. General procedure for synthesis of Cu(II) complexes

To a magnetically and refluxed solution of the ligands (0.001 mol) in DMF solution (30 ml), a solution of $CuCl_2.2H_2O$ (0.002 mol) in ethanol (10 ml) was added. The resulting mixtures were filtered and reduced to half of their volume by evaporation of the solvent. The concentrated solutions were left overnight at room temperature, which led to the formation of a solid product. They were filtered off, washed with a small amount of ether and dried over anhydrous $CaCl_2$.

2.5. Molecular modeling studies

An attempt to gain a better insight on the molecular structure of Metal complexes, geometric optimization and conformational analysis has been performed by the use of MM+ force field as implemented in hyperchem 8.0 [30]. Semi empirical method PM3 is then used for optimizing the full geometry of the system using Polak–Ribiere (conjugate gradient) algorithm and Unrestricted Hartee–Fock (UHF) is employed keeping RMS gradient of 0.01 kcal/mol. All the calculations refer to isolated molecules in vacuum.

2.6. Antibacterial studies

The in vitro antimicrobial activity of some selected compounds has been investigated using a modified Kirby–Bauer disc diffusion method [31]. Briefly, 100 μl of the test bacteria/fungi were grown in 10 ml of fresh media until they reached 108 cells/ml for bacteria or 105 cells/ml for fungi [32]. 100 μl of microbial suspension was spread onto agar plates corresponding to the broth in which they

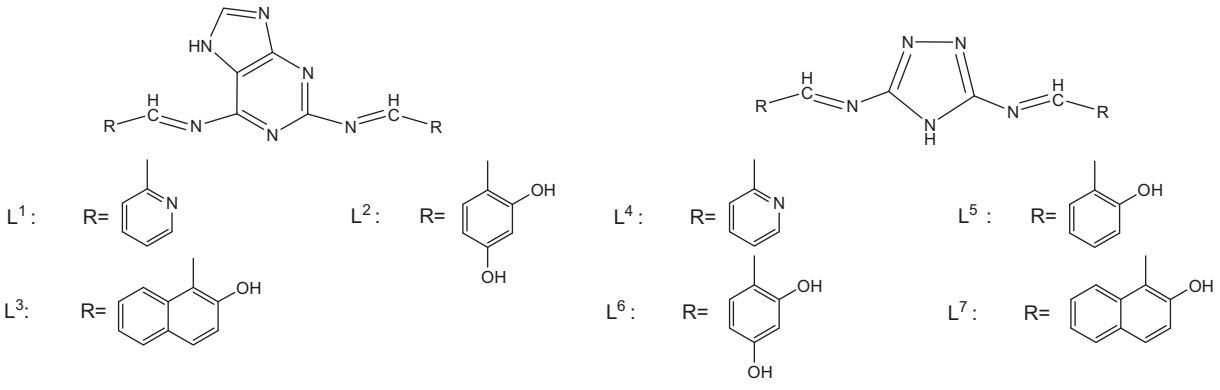

Fig. 1. A schematic representation of ligands used for the syntheses of Cu(II) complexes.

were maintained. Isolated colonies of each organism that might be playing a pathogenic role should be selected from primary agar plates and tested for susceptibility by disc diffusion method [33]. From the many media available, NCCLS recommends Mueller–Hinton agar since it results in good batch-to-batch reproducibility and also it is non-selective and non-differential medium which means that almost all organisms plated on here will grow. Disc diffusion method for filamentous fungi tested by using approved standard method (M38-A) developed by the NCCLS [34] for evaluating the susceptibilities of filamentous fungi to antifungal agents. Disc diffusion method for yeasts developed by using approved standard method (M44-P) by the NCCLS [35]. The antibacterial and antifungal activities were done at concentration of 1 mg/ml of the tested compounds in DMSO solvent. Plates inoculated with filamentous fungi as *Aspergillus flavus NRRL 6554* at 25 °C for 48 h; Gram positive bacteria as *Staphylococcus aureus NCTC 6356* and Gram negative bacteria as *Escherichia coli NRRL-B-3704*. They were incubated at 35–37 °C for 24–48 h and yeast as *Candida albicans ATCC 10231* incubated at 30 °C for 24–48 h and, then the diameters of the inhibition zones were measured in millimeters [36]. Standard discs of tetracycline (antibacterial agent) and amphotericin B (antifungal agent) served as positive controls for antimicrobial activity but filter discs impregnated with 10 μl of solvent (distilled water, DMSO) were used as a negative control. The agar used is Mueller–Hinton agar that is rigorously tested for composition and pH. Further the depth of the agar in the plate is a factor to be considered in the disc diffusion method. This method is well documented and standard zones of inhibition have been determined for susceptible and resistant values. Blank paper disks (Schleicher & Schuell Spain) with a diameter of 8.0 mm were impregnated 10 μl of tested concentration of the stock solutions. When a filter paper disc impregnated with a tested chemical is placed on agar the chemical will diffuse from the disc into the agar. This diffusion will place the chemical in the agar only around the disc. The solubility of the chemical and its molecular size will determine the size of the area of chemical infiltration around the disc. If an organism is placed on the agar it will not grow in the area around the disc if it is susceptible to the chemical. This area of no growth around the disc is known as a "Zone of inhibition" or "Clear zone". For the disc diffusion, the zone diameters were measured with slipping calipers of the National Committee for Clinical Laboratory Standards [36].

2.7. Measurement of potential cytotoxicity by SRB assay

Three human cancer cell lines were used for in vitro screening experiments; *breast cancer* (MCF7), *colon carcinoma* (HCT116) and *liver Carcinoma* (HEPG2) cell lines. They were obtained frozen in liquid nitrogen (−180 °C) from the American Type Culture Collection. The tumor cell lines were maintained in the National Cancer Institute, Cairo, Egypt, by serial sub-culturing. Potential cytotoxicity of the compounds was tested using Skehan et al. method [37]. Cells were plated in 96-multiwell plate (104 cells/well) for 24 h before treatment with the compound to allow attachment of cell to the wall of the plate. Different concentration of the compounds under test (0, l, 2.5, 5, l0, 15, 20 and 50 μg/ml) were added to the cell monolayer triplicate wells were prepared for each individual dose. Monolayer cells were incubated with the compounds for 48 h at 37 °C and in atmosphere of 5% CO_2. After 48 h, Cells were fixed, washed and stained with Sulfo-Rhodamine-B stain. Excess stain was washed with acetic acid and attached stain was recovered with Tris EDTA buffer. Color intensity was measured in an ELISA reader. The relation between surviving fraction and drug concentration is plotted to get the survival curve of each tumor cell line after the specified compound. An Elisa reader (TECAN SUNRISE), Potential cytotoxicity of the compounds was measured in (Pharmacology Unit, Cancer Biology Department, National Cancer Institute, Cairo University). Doxorubicin was used as standard cytotoxins.

3. Results and discussion

3.1. Molar conductivity measurements

The molar conductance values of 10^{-3} M solution of the metal complexes in DMF were calculated at room temperature (Table 1). The non-electrolytic nature of the metal complexes was confirmed by the low molar conductance values measured for DMF solution of the compounds [38] (Λ_M = 12.6–22.9 Ω^{-1} cm^2 mol^{-1}).

3.2. ^{1}H NMR spectra of the ligands

^{1}H NMR spectra of the Schiff bases (L^1–L^7) were recorded in d^6-DMSO (Table 2). The ^{1}H-NMR spectra of the ligands exhibited a multiple within the range 6.72–8.34 ppm which assigned to aromatic protons. The azomethine protons (—CH=N—) appeared as a singlet at 8.92–9.51 ppm. All the ligands, except L^1 and L^4, showed a peak at 10.34–11.21 ppm, belonging to the phenolic OH protons [39]. The most downfield signals observed as a singlet is due to NH protons of purine and triazole moieties and appeared at 12.81–13.87 [40].

3.3. IR spectra

Verification of the structure of metal complexes can be easily achieved by comparing the IR spectra of the free ligands with their metal complexes (Table 2). Such comparison revealed that the absorption band appearing in the ligands spectra at 1617–1573 cm^{-1} due to the azomethine group is shifted to lower or higher wavenumbers by 8–26 cm^{-1} in the complexes spectra, suggesting coordination through the azomethine nitrogen [41]. On the other hand, the ligand band at 1655–1617 cm^{-1} which assigned to υ(C=N) of the ring appears, almost at the same position, in the spectra of complexes. In the case of complexes **1** and **4**, this band is shifted to lower wanvenumbers revealing the coordination of the C=N of pyridine ring to the copper ion. These observations are supported by the appearance of a non-ligand bands at 480–407 cm^{-1}, which were tentatively assigned to the ν(M—N) mode [42]. The phenolic C—O of the free ligands is observed at 1299–1239 cm^{-1} [43]. Upon chelation, this band is shifted to lower or higher values by 10–47 cm^{-1} indicating the participation of the oxygen atom of phenolic group in coordination to the metal ion. Moreover, according to properties of non-electrolytic nature of the metal complexes, it can be inferred that deprotonated phenolic oxygen coordinates to metal ions due to the satisfaction of the bivalency of the metal ions. The new bands appearing at 589–512 cm^{-1} assigned to ν(M—O) band [42]. The appearance of a broad band within 3463–3385 cm^{-1} range in the spectra of hydrated complexes are assigned to ν(OH) of water molecules attached to the metal center.

3.4. EI-mass spectra

The constitutions and purities of the prepared complexes are confirmed using the electron impact mass spectrometry. Fig. 2 represents the mass spectrum of complex **1**, as a representative example. The mass spectrum of this complex [$Cu_2L^1Cl_3$], showed a peak at m/z 560 corresponding to the molecular ion peak of the compound. The peaks observed at m/z 491 and 453 assigned to [Cu_2L^1Cl] and [Cu_2L^1], respectively. The intensity ratios of the observed peaks around 560, 490 and 453 are consistent with the isotopic distributions for Cu_2Cl_3, Cu_2Cl and Cu_2 containing

Table 1
Analytical and physical data of organic ligand and their metal complexes.

No.	Compound (Empirical formula)	Color (Λ_m)[a]	m.p (°C) (%Yield)	M. Wt.	Elemental analysis found (Calc.)			
					%C	%H	%N	%M
L^1	$C_{17}H_{12}N_8$	Faint yellow	250	328.33	62.63	3.27	34.55	–
		(–)	71		(62.19)	(3.68)	(34.13)	
L^2	$C_{19}H_{14}N_6O_4$	Orange	280	390.35	58.13	3.74	21.84	–
		(–)	64		(58.46)	(3.61)	(21.53)	
L^3	$C_{27}H_{18}N_6O_2$	Orange	>300	458.47	70.27	3.84	18.24	–
		(–)	77		(70.73)	(3.96)	(18.33)	
L^4	$C_{14}H_{11}N_7$	Greenish yellow	>300	277.28	60.33	3.79	35.64	–
		(–)	72		(60.64)	(4.00)	(35.36)	
L^5	$C_{16}H_{13}N_5O_2$	Deep yellow	293	307.31	62.87	4.44	22.42	–
		(–)	84		(62.53)	(4.26)	(22.79)	
L^6	$C_{16}H_{13}N_5O_4$	Orange	>300	339.31	56.35	3.54	20.39	–
		(–)	66		(56.64)	(3.86)	(20.64)	
L^7	$C_{24}H_{17}N_5O_2$	Yellow	277	407.42	70.57	3.95	17.32	–
		(–)	78		(70.75)	(4.21)	(17.19)	
1	$[Cu_2L^1Cl_3]$	Greenish grey	>300	560.77	36.61	2.23	19.63	22.36
	($C_{17}H_{11}Cl_3Cu_2N_8$)	(18.6)	68		(36.41)	(1.98)	(19.98)	(22.66)
2	$[Cu_2L^2Cl_2(H_2O)_2]$	Greenish grey	>300	622.36	36.23	2.81	13.62	20.18
	($C_{19}H_{16}Cl_2Cu_2N_6O_6$)	(12.6)	67		(36.67)	(2.59)	(13.50)	(20.42)
3	$[Cu_2L^3Cl_2(H_2O)_2]$	Brown	>300	690.48	47.27	2.72	12.54	18.10
	($C_{27}H_{20}C_{l2}Cu_2N_6O_4$)	(13.7)	71		(46.97)	(2.92)	(12.17)	(18.41)
4	$[Cu_2L^4Cl_4](H_2O)_2$	Green	>300	582.22	28.59	2.24	16.52	21.64
	($C_{14}H_{15}Cl_4Cu_2N_7O_2$)	(22.9)	65		(28.88)	(2.60)	(16.84)	(21.83)
5	$[Cu_2L^5Cl_2(H_2O)_2]$	Brown	>300	539.32	35.27	2.57	13.20	23.16
	($C_{16}H_{15}Cl_2Cu_2N_5O_4$)	(15.8)	69		(35.63)	(2.80)	(12.99)	(23.57)
6	$[Cu_2L^6Cl_2(H_2O)_2]$	Brown	>300	571.32	33.89	2.12	12.49	22.81
	($C_{16}H_{15}Cl_2Cu_2N_5O_6$)	(12.9)	64		(33.64)	(2.65)	(12.26)	(22.25)
7	$[Cu_2L^7Cl_2(H_2O)_2]0.5H_2O$	Deep brown	162	648.44	44.56	3.25	11.31	19.37
	($C_{24}H_{20}Cl_2Cu_2N_5O_{4.5}$)	(14.2)	66		(44.45)	(3.11)	(10.8)	(19.60)

[a] (Ω^{-1} mol^{-1} cm^2).

Table 2
IR and ^{1}H NMR spectral bands of the ligands and their Cu(II) complexes.

Comp.	IR spectra (cm^{-1})							^{1}H NMR spectra (ppm)			
	ν(OH) or ν(H_2O)	ν(NH)	ν(C=N) (ring)	ν(C=N) (imine)	ν(C—O)	ν(M—O)	ν(M—N)	$\delta_{\underline{H}N}$	$\delta_{O\underline{H}}$	$\delta_{C\underline{H}=N}$	$\delta_{Ar-\underline{H}}$
L^1	–	3363	1655	1600	–	–	–	13.68	–	9.35	7.21–7.92
1	–	–	1638	1592	–	–	480	–	–	–	–
L^2	3463	3357	1649	1617	1239	–	–	13.87	10.85, 10.34	9.12	
2	3386	3323	1647	1593	1221	520	453	–	–	–	–
L^3	3423	3318	1655	1595	1299	–	–	12.98	10.56	9.39	7.44–8.34
3	3400	3313	1655	1611	1289	589	477	–	–	–	–
L^4	–	3311	1617	1580	–	–	–	12.95	–	8.92	6.72–7.81
4	3366	3237	1596	1560	–	–	413	–	–	–	–
L^5	3385	3312	1644	1573	1274	–	–	12.81	11.21	9.51	6.95–7.84
5	3398	3329	1644	1555	1232	512	463	–	–	–	–
L^6	3459	3344	1629	1585	1261	–	–	13.41	10.91, 10.52	9.32	6.81–7.92
6	3397	3301	1630	1611	1297	547	407	–	–	–	–
L^7	3430	3200	1631	1583	1245	–	–	12.98	11.21	9.22	7.35–8.32
7	3417	3244	1629	1609	1292	523	455	–	–	–	–

compounds, respectively (Fig. 2(a–c)). The loss of the chlorine atoms confirm that the chlorine atom attached to the metal ion with a covalent bond [44]. For the other metal complexes, the peaks observed at m/z 622, 690, 582, 539, 571 and 648 for complexes 2, 3, 4, 5, 6 and 7 respectively, corresponded to the molecular ion peak of these complexes. The results of both elemental analyses and MS of the prepared complexes are in satisfactory agreement with each other's which confirm the proposed molecular formula (Table 1).

3.5. Thermal behavior of metal complexes

The thermal behavior of some selected metal complexes was characterized on the basis of TG and DTA methods. Thermoanalytical data of the complexes are given in Table 3; the TG/DTA thermograms of complexes **2** and **4**, as representative examples, are represented in Fig. 3. From this table it is clear that all the metal complexes underwent thermal decomposition within three or four steps. The Cu(II) complex **2** decomposed in four steps. The first step occurred within the range 37–145 °C and corresponded to the loss of coordinated water molecules. This step associated with endothermic DTA peak at 102 °C. The second and third steps of decomposition appeared within the temperature ranges 145–239 and 239–385 °C and corresponded to the loss of coordinated chloride ions and partial decomposition of the ligand with the loss of two —OH groups. These step associated with exothermic DTA peak with maximum at 218 °C. The organic ligand was further decomposed within the temperature range 385–576 °C leaving behind CuO as final product.

The Cu(II) complexes **4** decomposed in four steps. The first step occurred within the range 34–115 °C and corresponded to the loss of lattice water molecule. This step of decomposition associated

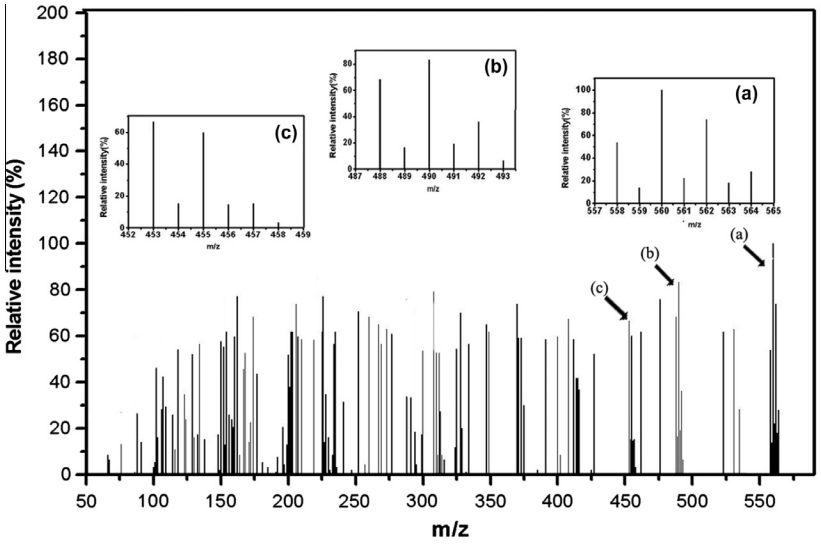

Fig. 2. Mass spectra of complex **1**.

Table 3
Thermal analyses (DTA and TGA) of the metal complexes.

No.	Complex	TG range (°C)	DTA max (°C)	(Calc.) found mass loss %	assignment
2	$[Cu_2L^2Cl_2(H_2O)_2]$	37–145	102(−)	(5.78) 5.91	– Loss of two coordinated water
	(622.36)	145–239	218(+)	(5.70) 5.44	– Loss of one coordinated chloride ion
		239–385	–	(11.16) 11.77	– Loss of one coordinated chloride ion with two —OH
		385–576	540(−)	(51.51) 51.57	– Further decomposition of ligand leaving CuO residue
4	$[Cu_2L^4Cl_4](H_2O)_2$	34–115	55(−)	(3.09) 2.84	– Loss of one lattice water
	(582.22)	115–257	189(+)	(9.18) 8.98	– Loss of one lattice water and one coordinated chloride
		257–344	255(−)	(18.29) 17.93	– Loss of 3 coordinated chloride ions
		344–550	538(+)	(47.62) 47.14	– decomposition of ligand leaving CuO residue
5	$[Cu_2L^5Cl_2(H_2O)_2]$	31–150	112(−)	(6.67) 6.85	– Loss of two coord. H_2O
	(539.32)	150–264	214(+)	(25.41) 25.79	– Loss of two coord. Cl^- and triazole ring
		264–380	280(+)	(10.01) 9.76	– loss of two azomethine groups
		380–538	416(+)	(28.22) 28.63	– further decomposition of ligand leaving CuO residue
6	$[Cu_2L^6Cl_2(H_2O)_2]$	31–147	104(−)	(6.30) 6.06	– Loss of two coord. H_2O
	(571.32)	147–311	230(+)	(12.42) 12.98	– Loss of two coord. Cl^-
		311–616	290(+)	(53.38) 53.21	– decomposition of ligand leaving CuO residue
7	$[Cu_2L^7Cl_2(H_2O)_2]0.5H_2O$	31–104	98(−)	(1.38) 1.55	– Loss of lattice water
	(648.44)	104–388	–	(16.50) 16.21	– Loss of coordinated water and chloride
		388–629	395(+)	(57.58) 57.89	– decomposition of ligand leaving CuO residue

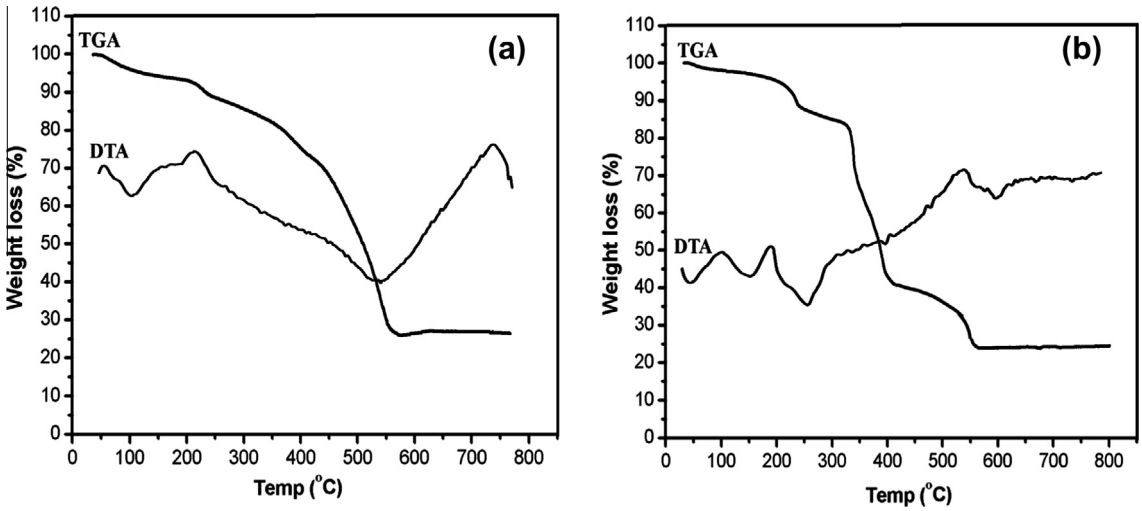

Fig. 3. TG/DTA thermograms of complex 2 (a) and complex 4 (b).

with endothermic DTA peak at 55 °C. The second step of decomposition appeared within the temperature range 115–257 °C and corresponded to the loss of one lattice water and one coordinated chloride ion. This step associated with exothermic DTA peak at 189 °C. The third step occurred at 257–344 °C and corresponded to the loss of coordinated chloride ion with endothermic DTA peak at 255 °C. The last step appeared at 344–550 °C and corresponded to decomposition of the organic ligand with the formation of CuO as final product. This step associated with exothermic DTA peak at 538 °C.

For the complexes **5** and **6**, the first step of decomposition occurred within the ranges 31–150 and 31–147 °C, respectively, and corresponded to the loss of coordinated water molecules. These steps accompanied with DTA peaks at 112 and 104 °C for complexes **5** and **6**, respectively. The second step of decomposition appeared at 150–264 and 147–311 °C associated with DTA peak at 214 and 230 °C for the complexes **5** and **6**, respectively. This step of decomposition corresponded to the loss of coordinated chloride ions. Complex **5** further decomposed in two steps within the range 264–380 and 380–538 °C associated with DTA peaks at 280 and 416 °C while the last step of decomposition for complex 6 appeared at 311–616 °C with DTA peak at 290 °C resulting in the formation of CuO as final product.

Complex **7** decomposed in three steps, the first step appeared at 31–104 °C and corresponded to the loss of lattice water with endothermic DTA peak at 98 °C. The second step of decomposition appearing at 104–388 °C assigned to the loss of coordinated water and chloride. The third step appeared at 388–629 °C corresponding to the decomposition of the organic ligand with the formation of CuO as final product. This step accompanied with exothermic DTA peak at 395 °C. As shown in Table 3, the calculated mass loss of each step of decomposition is in a good agreement with the found ones which confirm the proposed structures.

3.6. Magnetic moments and electronic spectra

The information regarding the geometry of the metal complexes was obtained from their electronic spectral data and magnetic moments. The UV–Vis spectral data of all the metal complexes are given in Table 4. The electronic spectral data of complexes **2**, **3**, **5**, 6 and **7** in the solid state showed three absorption bands above 300 nm, centered approximately within the ranges 370–400, 480–485 nm and 632–645 nm. The absorption within the range 480–485 nm is likely to be due to charge transfer from the nitrogen atoms to the copper ions [45]. The broad band appearing at 632–645 nm is identified to the complex itself with d–d electronic ($^2T_2 \rightarrow {}^2E$) transitions [46,47] assuming distorted tetrahedral geometry around Cu(II). In the case of square planar copper complexes, three allowed transitions are expected in the visible region, but often these theoretical expectations are overlooked in practice, and these bands usually appear overlapped as a broad flap band due to the very small energy difference between the d levels [48]. The electronic spectra of the Cu(II) complexes **1** and **4** showed a broad band appearing at 680 and 665 nm for **1** and **4**, respectively, due to the d–d ($B_{1g} \rightarrow A_{1g}$) transition expected for square planar Cu (II) complexes [49,50]. The two bands appearing at 420 & 509 nm for complex **1** and 420 & 480 nm for complex **4** were assigned to charge transfer transitions. The medium intensity band appearing at 345 and 350 nm for complexes **1** and **4**, respectively, is also indicative for a four-coordinated square planar geometry of Cu(II) [51,52]. The two bands appearing at 220 & 240 nm and 222 & 261 nm for complexes **1** and **4**, respectively, assigned to intraligand charge transfer transitions. The geometries around the metal centers were further confirmed by the ESR data.

The magnetic values of the complexes lay within the range 1.21–1.39 B.M. The subnormal, very low, magnetic moment values of the metal complexes indicated that the copper centers are antiferromagnetically coupled [53].

3.7. ESR spectra

Based on hyperfine and super hyperfine structures, the ESR spectrum of metal complexes provides information about the environment of the metal ion within the complexes, *i.e.*, the geometry and nature of the legating sites of the Schiff base and the metal. The ESR spectra of the Cu(II) complexes **2**, **4**, **5** and **7** were recorded at room temperature. The shift of the signal in the low-field region to a slightly lower value indicates stronger metal–ligand bonding [54]. The Cu(II) chelates **4** and **7** showed two peaks, one in the low field region and the other in the high field region, from which g_{ll} and $g_{\perp}$ were calculated (Table 4). The g_{ll} values (<2.3) indicate covalent character of the metal–ligand bonds [55]. The covalent nature of the metal–ligand bond in the complex is further supported by the g_{eff} value [56], which was <2.0023. The value $g_{ll} > g_{\perp}$ is well consistent with a primarily dx^2–y^2 ground state [57]. The $d_{X^2-Y^2}$ G.S. is characteristic of square planer, square pyramidal, tetrahedral or octahedral sterochemistry [58]. The g_{ll}/A_{ll} value can be used to determine the stereochemistry of the copper (II) complex [59]. The range reported for square planar complexes is 105–135 cm^{-1} and for tetrahedrally distorted complexes 150–250 cm^{-1}. The g_{ll}/A_{ll} value is 111 cm^{-1} for complex **4** in the range of square planar and 187 cm^{-1} for complex **7** in the range expected for distorted tetrahedral complexes.

The ESR spectra of the other Cu (II) complexes (**2** and **5**) display a small broad signal. The g_{eff} values are 1.72 and 1.68 for complexes **2** and **5**, respectively. The negative deviation of g_{eff} value from the value of the free electron (g_{eff} = 2.0023) may be attributed to covalent character of the bond between the Cu(II) ion and the ligand molecule [60]. The apparent broadening of the ESR signal can be due to antiferromagnetic interaction of Cu—Cu ions.

3.8. Molecular modeling

Since our trials to obtain a single crystals of the metal complexes were unsuccessful so far, and in order to gain a better understanding of geometrical structures of the investigated complexes, molecular modeling studies have been done by means of Hyperchem program package. Some selected bond lengths and angles are listed in Table 5; the optimized structures, with atom labeling scheme, of complexes **1** and **6** are represented in Figs. 4

Table 4
Magnetic moment, electronic and ESR spectral data of metal complexes.

Comp.	λ (nm)	μeff (B.M.)	g_{ll}	$g_{\perp}$	g_{ll}/A_{ll}	g_{eff}
1	220, 240, 345, 420, 509, 680	1.39				
2	380, 485, 625	1.34				1.72
3	370, 480, 640	1.21				
4	222, 261, 350, 420, 480, 665	1.31	2.00	1.79	111	
5	385, 480, 640	1.34				1.68
6	370, 485, 632	1.26				
7	400, 480, 635	1.24	1.87	1.70	187	

Table 5
Some selected bond distances (A°) and bond angles (°) of metal complexes.

Bond	Length (A°)	Bond	Angle (°)	Bond	Length (A°)	Bond	Angle (°)
Complex 1				Complex 5			
N1—Cu2	1.8746	N1Cu2 Cl10	91.60	N8—Cu9	1.9359	N8Cu9 O10	98.49
Cu2—Cl10	2.1395	N1Cu2 Cl11	177.39	Cu9—O10	1.8980	N8Cu9 Cl28	108.89
Cu2—Cl11	2.1550	N1Cu2 N3	92.16	Cu9—Cl28	2.2388	N8Cu9 O29	119.18
Cu2—N3	1.8765	Cl10Cu2Cl11	85.88	Cu9—O29	1.9570	O10Cu9Cl28	114.70
N12—Cu27	1.8727	Cl10Cu2N3	175.27	N16—Cu21	1.9179	O10Cu9O29	104.59
N24—Cu27	1.8728	Cl11Cu2N3	90.39	O20—Cu21	1.8969	Cl28Cu9O29	110.63
C25—C26	1.4388	N12Cu27N24	175.92	Cu21—Cl26	2.1992	N16Cu21O20	98.57
C25—C29	1.3715	N12Cu27Cl30	90.31	Cu21—O27	1.9608	N16Cu21Cl26	129.35
Cu27—Cl30	2.1662	N12Cu27N28	91.59	C7—N8	1.3301	N16Cu21O27	112.98
Cu27—N28	1.8725	N24Cu27Cl30	93.08	N16—C17	1.3282	O20Cu21Cl26	111.43
N28—C29	1.4146	N24Cu27N28	85.09	C3—C4	1.3641	O20Cu21O27	103.21
N1—C5	1.3122	Cl30Cu27N28	177.53	C2—O10	1.3044	Cl26Cu21O27	99.05
Complex 2				Complex 6			
C1—C2	1.4404	O7Cu8Cl11	103.90	N8—Cu9	1.9362	N8Cu9 O10	98.31
C1—C6	1.3529	O7Cu8O12	97.76	Cu9—O10	1.8989	N8Cu9 Cl28	108.93
O7—Cu8	1.8987	O7Cu8N9	100.20	Cu9—Cl28	2.2382	N8Cu9 O29	119.20
Cu8—Cl11	2.1935	Cl11Cu8O12	92.01	Cu9—O29	1.9567	O10Cu9Cl28	114.64
Cu8—O12	1.940	Cl11Cu8N9	146.48	N16—Cu21	1.9187	O10Cu9O29	104.62
Cu8—N9	1.8960	O12Cu8N9	107.52	O20—Cu21	1.8981	Cl28Cu9O29	110.73
N13—Cu15	1.8714	N13Cu15O16	95.94	Cu21—Cl26	2.2000	N16Cu21O20	98.40
Cu15—O16	1.8433	N13Cu15O25	121.13	Cu21—O27	1.9608	N16Cu21Cl26	129.29
Cu15—O25	1.9362	N13Cu15Cl26	142.67	C7—N8	1.3306	N16Cu21O27	112.84
Cu15—Cl26	2.2230	O16Cu15O25	89.51	N16—C17	1.3293	O20Cu21Cl26	111.53
N1—C19	1.3119	O16Cu15Cl26	88.97	C3—C4	1.3751	O20Cu21O27	103.42
N9—C10	1.3694	O25Cu15Cl26	95.82	C4—O34	1.3664	Cl26Cu21O27	99.20
Complex 3				Complex 7			
O7—Cu8	1.9141	O7Cu8Cl11	108.48	N8—Cu9	1.8627	N8Cu9O10	100.37
Cu8—Cl11	2.2515	O7Cu8O12	104.60	N8—C11	1.4493	N8Cu9Cl28	150.23
Cu8—O12	1.9423	O7Cu8N9	100.75	Cu9—O10	1.8559	N8Cu9O29	113.46
Cu8—N9	1.9446	Cl11Cu8O12	108.73	Cu9—Cl28	2.1874	O10Cu9Cl28	95.50
N13—Cu14	1.8772	Cl11Cu8N9	113.48	Cu9—O29	1.9788	O10Cu9O29	100.56
Cu14—O15	1.8375	O12Cu8N9	119.60	C11—N12	1.5112	Cl28Cu9O29	87.84
Cu14—O23	1.9126	N13Cu14O15	95.68	N16—Cu21	1.8627	N16Cu21O20	100.36
Cu14—Cl24	2.2184	N13Cu14O23	118.50	O20—Cu21	1.8559	N16Cu21Cl26	150.22
N9—C10	1.4081	N13Cu14Cl24	131.55	Cu21—Cl26	2.1874	N16Cu21O27	113.52
N13—C18	1.3070	O15Cu14O23	88.91	Cu21—O27	1.9787	O20Cu21Cl26	95.51
C1—C6	1.3623	O15Cu14Cl24	87.33	C22—C23	1.3920	O20Cu21O27	100.45
C3—C4	1.4641	O23Cu14Cl24	109.89	C23—C24	1.4215	Cl26Cu21O27	87.82
Complex 4							
N1—C5	1.4599	N7Cu8 N9	91.56				
N7—Cu8	1.8758	N7Cu8 Cl26	178.51				
Cu8—N9	1.8766	N7Cu8 Cl27	92.96				
Cu8—Cl26	2.1585	N9Cu8 Cl26	89.84				
Cu8—Cl27	2.1493	N9Cu8 Cl27	173.00				
N18—Cu19	1.8762	Cl26Cu8Cl27	85.70				
Cu19—Cl24	2.1486	N6Cu19N18	91.57				
Cu19—Cl25	2.1582	N6Cu19Cl24	93.12				
C20—C21	1.3742	N6Cu19Cl25	178.44				
C21—C22	1.4083	N18Cu19Cl24	172.63				
C22—C23	1.3781	N18Cu19Cl25	89.84				
N9—C10	1.3867	Cl24Cu19Cl25	85.55				

and 5. The complexes feature four-coordinated Cu centers with NN, NNN (complexes 1 and 4) and NO (complexes 2, 3, 5, 6, and 7) donor set of the Schiff base ligands.

For complexes **1** and **4**, the copper atom is situated almost exactly on the average plane defined by the donor atoms of the ligands and chloride ions. The cis angles around the Cu(II) ion range from 85.09° to 93.08° and from 85.55° to 93.12° for complexes **1** and **4**, respectively; the trans angles ranging from 175.27° to 177.53° and from 172.63° to 178.51° for complexes **1** and **4**, respectively, indicating square planar geometry with almost no tetrahedral distortion [61,62].

For complexes **2**, **3**, **5**, **6** and **7**, the dihedral coordination around the Cu(II) center, involving O, N and Cl atoms is distorted. The degree of distortion from ideal tetrahedral geometry is given by the minimum and maximum coordination angles around Cu. For complexes **2**, **3**, **5**, **6** and **7**, the minimum angles are 88.97, 87.33, 98.49, 98.31 and 87.82, respectively. The maximum angles are 123.40, 131.55, 129.35, 129.29 and 150.23 for complexes **2**, **3**, **5**, **6** and **7** respectively. From Table 5, it is clear that the bond lengths are found to be within the normal ranges obtained from the crystal structure data [63]. The obtained results are in a good agreement with the experimental results and hence strongly support them.

3.9. Antibacterial results

Taking into account the daily necessary quantity of Cu(II) in the organism (2–3 mg per day), its distribution and metabolism in the organism and toxicity, numerous simple or complex combinations of copper are used in the treatment of a variety of diseases, including inflammatory processes, cancer, ulcers, nervous system, and heart diseases [28]. Some selected ligands, namely L^1, L^2, L^5 and L^6, and their complexes were screened for their antibacterial activity against *E. coli* (G^-) and *S. aureus* (G^+) and antifungal activity against *A. flavus* and *C. albicans*. The standard drugs, tetracycline

and amphotericin B, were also tested for their antibacterial and antifungal activities at the same concentration (1 mg/ml) and conditions of the test compounds (Table 6). From the obtained data, the following results are pointed out:

1. All the tested compounds, except for complex **2**, are found to have no biological activity against *A. flavus*.
2. With *C. albican*, L^2, complex **2** and **6** showed moderate activity while the other compounds showed no activity.
3. All the tested compounds showed a moderate activity against the bacterial strains *E. coli* and *S. aureus*, except for L^1 which is inactive against the both types of bacteria.
4. On comparing the activity of the tested complexes with their parent ligands, the obtained data indicated that the activity is increased upon complexation (except for L^2 and complex **2** against *S. aureus* and *C. albicans*). This result may be explained by on the basis of chelating theory [64], which stated that chelating reduces the polarity of the ligand and the central metal

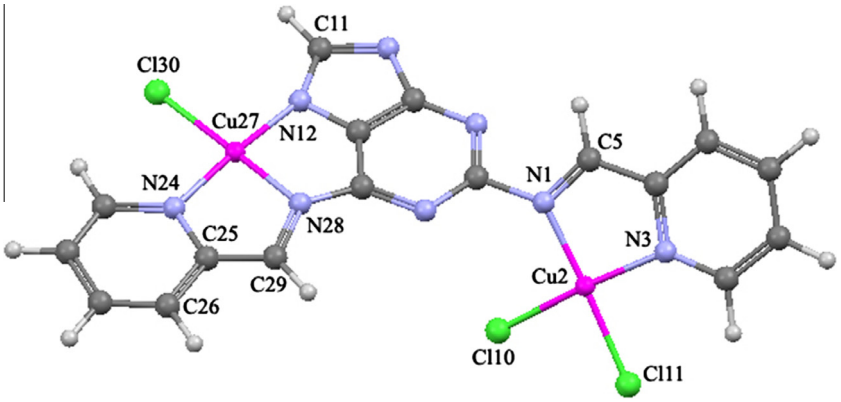

Fig. 4. Computational structure of complex 1.

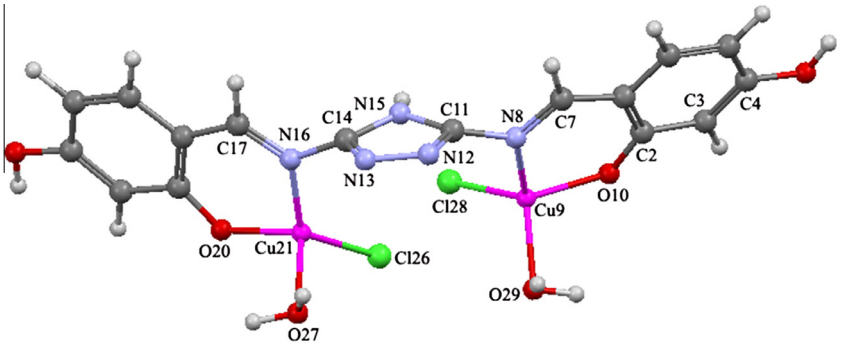

Fig. 5. Computational structure of complex 6.

Table 6
Antimicrobial activities of the investigated ligands and their Cu(II) complexes.

Compound	Inhibition zone diameter (mm/mg sample)[a]			
	E. coli (G^-)	*S. aureus* (G^+)	*A. flavus* (Fungus)	*C. albicans* (Fungus)
Control: DMSO	NA[b]	NA	NA	NA
Tetracycline[c]	33.0 ± 0.3	30.0 ± 0.4	–	–
Amphotericin B[d]	–	–	20.0 ± 0.2	20.0 ± 0.1
L^1	NA	NA	NA	NA
1	12.0 ± 0.3	12.0 ± 0.2	NA	NA
L^2	12.0 ± 0.3	13.0 ± 0.2	NA	17.0 ± 0.2
2	13.0 ± 0.3	12.0 ± 0.2	16.0 ± 0.4	11.0 ± 0.2
L^5	12.0 ± 0.3	13.0 ± 0.4	NA	NA
5	13.0 ± 0.4	14.0 ± 0.2	NA	NA
L^6	11.0 ± 0.2	12.0 ± 0.3	NA	NA
6	15.0 ± 0.5	15.0 ± 0.4	NA	12.0 ± 0.3

[a] Diameter of zone of inhibition (mm) including well diameter 8 mm, each experiment has been conducted three times at least.
[b] Not active.
[c] (Antibacterial agent).
[d] (Antifungal agent).

Table 7
In vitro antitumor activities of complex 2 against MCF7, HCT116 and HEPG2 cell lines.

Compound	IC_{50} (μg/ml)		
	MCF7	HCT116	HEPG2
2	10.3	9.8	8.7
Dox[a]	4.35	4.6	3.1

[a] Doxorubicin, standard cytotoxin drug.

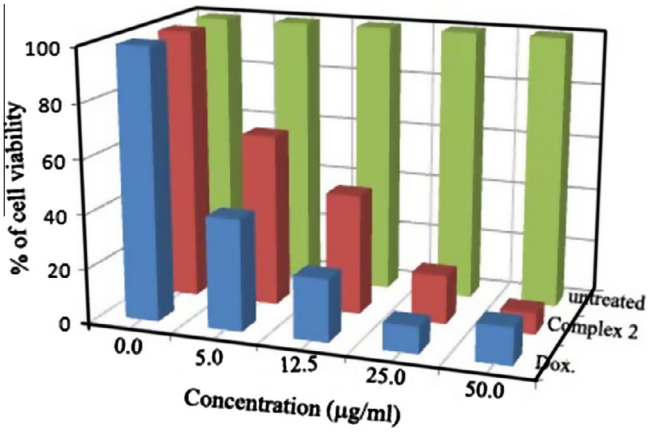

Fig. 6. In vitro cytotoxicity of 2 and doxorubicin (Dox) drug against human breast cancer cell line (MCF7).

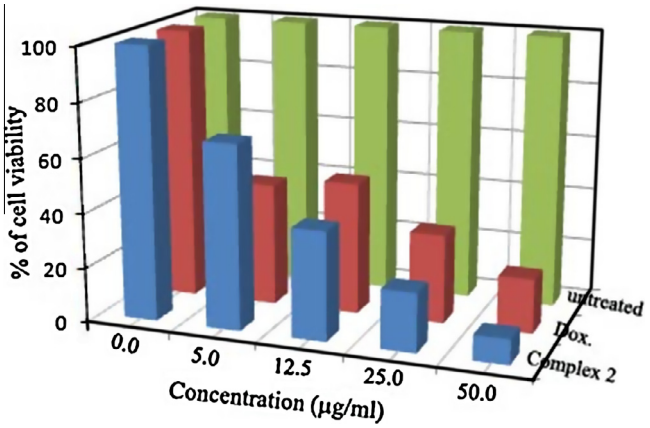

Fig. 7. In vitro cytotoxicity of 2 and doxorubicin (Dox) drug against human colon carcinoma (HCT116).

atom because the delocalization of π-electrons over the whole chelate ring increases, which favor permeation of the complexes through the lipid layer of the cell membrane.

5. Finally, the variation in the activity of different compounds against various organisms depends either on the impermeability of the cells of the microbes or differences in ribosome in microbial cells [65].

3.10. Antitumor results

In vitro antitumor activity of complex **2**, as a model example, against three cancer cell lines; *breast carcinoma* (MCF7), *colon carcinoma* (HCT116) and *liver Carcinoma* (HEPG2) cell lines was conducted in our study. The values of IC_{50}, compared with the

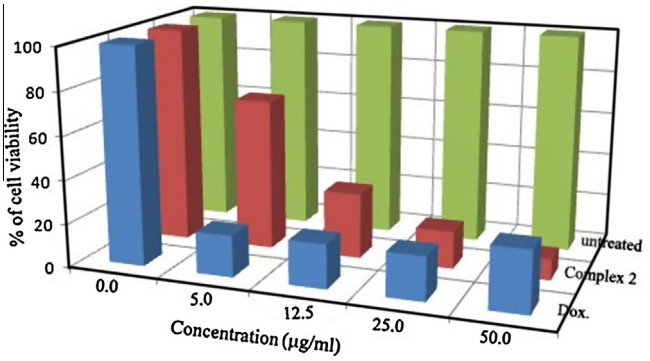

Fig. 8. In vitro cytotoxicity of 2 and doxorubicin (Dox) drug against against human liver Carcinoma (HEPG2).

standard drug doxorubicin are collected in Table 7 and revealed that compound **2** showed activity against all the tested cell lines. Figs. 6–8 represents the cytotoxicity of complex **2** and doxorubicin (Dox) drug against the three cell lines, using different concentrations of 2 or Dox. Untreated cells were used as a control. Each data point is an average of three independent experiments and expressed as M ± SD. From these figures it is clear that complex **2** inhibited the growth of the tested cells in a dose dependent manner. Specifically, compound **2** showed an inhibition of cell viability and gave an IC_{50} values of 10.3, 9.8 and 8.7 μg/ml against MCF7, HCT116 and HEPG2, respectively, compared with IC_{50} values of 4.6, 3.1, 4.35 against HCT116, HEPG2 and MCF7, respectively, for the standard cytotoxin drug doxorubicin. According to Shier [66], the compounds exhibiting IC_{50} activity within the range of 10–25 μg/ml are considered weak anticancer drugs, while those of IC_{50} activity between 5 and 10 μg/ml are moderate and compounds of activity below 5.00 μg/ml are considered strong agents. Accordingly, this complex showed a moderate activity against the studied cell lines; the order of activity is MCF7 > HCT116 > HEPG2.

4. Conclusion

In this study, seven new Cu(II) complexes with Schiff bases derived from 7*H*-2,6-diaminopurine and 4*H*-3,5-diamino-1,2,4-triazole were synthesized and characterized by elemental, mass spectra, thermal analyses, IR, spectral, and magnetic data. The electronic and ESR spectral studies suggested distorted tetrahedral geometry for all complexes, except for complex **1** and **4** which have square planar geometry. The obtained results are supported by 3D molecular modeling of complexes. The results of the antibacterial activity of the tested ligands and their complexes showed moderate activity against *E. coli* and *S. aureus* when compared with the standard drug, tetracycline. In vitro antitumor activity of complex **2** showed a moderate activity against the studied cell lines; the order of activity is MCF7 > HCT116 > HEPG2.

References

[1] X.F. Luo, X. Hu, X.Y. Zhao, S.H. Goh, X.D. Li, Polymer 44 (2003) 5285.
[2] A.S.N. Murthy, A.R. Reddy, J. Chem. Sci. 90 (1981) 519.
[3] V. Razakantoanina, N.K.P. Phung, G. Jaureguiberry, Parasitol. Res. 86 (2000) 665.
[4] R.E. Royer, L.M. Deck, T.J. Vander Jagt, J. Med. Chem. 38 (1995) 2427.
[5] M.R. Flack, R.G. Pyle, N.M. Mullen, J. Clin. Endocrinol. Metab. 76 (1993) 1019.
[6] R. Baumgrass, M. Weiwad, F. Erdmann, J. Biol. Chem. 276 (2001) 47914.
[7] N.A. Draanen, A. Freeman, S.A. Short, R. Harvey, R. Jansen, G. Szczech, G.W. Koszalka, J. Med. Chem. 39 (1996) 538.
[8] R.F. Pang, C.L. Zhang, D.K. Yuan, M. Yang, Bioorg. Med. Chem. 16 (2008) 8178.
[9] R.E. Colacio, J.D. lopez, J.M. Salas, Can. J. Chem. 61 (1983) 2506.
[10] K.A. Jacobson, P.J.M. Van Galen, M. Williams, J. Med. Chem. 35 (1992) 407.

[11] R.J. Griffin, C.E. Arris, C. Bleasdale, F.T. Boyle, A.H. Calvert, N.J. Curtin, C. Dalby, S. Kanugula, N.K. Lembicz, D.R. Newell, A.E. Pegg, B.T. Golding, J. Med. Chem. 43 (2000) 4071.
[12] M.E. Dolan, A.E. Pegg, Clin. Cancer. Res. 3 (1997) 837.
[13] A. Meerbach, J. Neyts, A. Holy, P. Wutzler, E.D. Clercq, Antivir. Chem. Chemother. 9 (1998) 275.
[14] M.H. Fleysher, R.J. Bernacki, G.A. Bullard, J. Med. Chem. 23 (1980) 1448.
[15] G. Vaidyanathan, D.J. Affleck, C.M. Cavazos, S.P. Johnson, S. Shankar, H.S. Friedman, M.O. Colvin, M.R. Zalutsky, Bioconjugate Chem. 11 (2000) 868.
[16] M. Belanich, M. Pastor, T. Randall, D. Guerra, J. Kibitel, L. Alas, B. Li, M. Citron, P. Wasserman, A. White, H. Eyre, K. Jaeckle, S. Shulman, D. Rector, M. Prados, S. Coons, W. Shapiro, D.B. Yarosh, Cancer Res. 56 (1996) 783.
[17] L. Harmse, R.V. Zyla, N. Grayb, S.P. Schultzb, L. Leclercc, C.D. Meijerc, I. Havlika, Biochem. Pharmacol. 62 (2001) 341.
[18] A.E. Gibson, C.E. Arris, J. Bentley, F.T. Boyle, N.J. Curtin, T.G. Davies, J.A. Endicott, B.T. Golding, S. Grant, R.J. Griffin, P. Jewsbury, L.N. Johnson, V. Mesguiche, D.R. Newell, M.E.M. Noble, J.A. Tucker, H.J. Whitfield, J. Med. Chem. 45 (2002) 3381.
[19] I. Bojidarka, Turk J. Chem. 31 (2007) 97.
[20] B.S. Holla, K.A. Poojary, B. Kalluraya, Farmaco 51 (1996) 793.
[21] S.N. Pandeya, D. Sriram, G. Nath, E. De Clercq, A. Forsch, Drug Res. 50 (2000) 55.
[22] F.P. Invidiata, S. Grimaudo, P. Giammanco, L. Giammanco, Farmaco 46 (1991) 1489.
[23] O.G. Todoulou, A. Papadaki-Valiraki, E.C. Filippatos, S. Ikeda, E. De Clercq, Eur. J. Med. Chem. 29 (1994) 127.
[24] M.H. Palmer, D. Christen, J. Mol. Struct. 705 (2004) 177.
[25] K. Singh, M.S. Barwa, P. Tyagi, Eur. J. Med. Chem. 41 (2006) 147.
[26] Z.H. Chohan, H. Pervez, A. Rauf, A. Scozzafava, C.T. Supuran, J. Enzyme Inhib. Med. Chem. 17 (2002) 117.
[27] J.E. Weder, C.T. Dillon, T.W. Hambley, B.J. Kennedy, P.A. Lay, Coord. Chem. Rev. 232 (2002) 95.
[28] A.M. Khedr, N.A. El-Wakiel, S. Jadon, V. Kumar, J. Coord Chem. 64 (5) (2011) 851.
[29] L. Tripathi, P. Kumar, A.K. Singhai, Indian J. Cancer 44 (2) (2007) 62.
[30] HyperChem Version 8.0 Hypercube, Inc.
[31] A.W. Bauer, W.M. Kirby, C. Sherris, M. Turck, Am. J. Clin. Path. 45 (1966) 493.
[32] M.A. Pfaller, L. Burmeister, M.A. Bartlett, M.G. Rinaldi, J. Clin. Microbiol. 26 (1988) 1437.
[33] National Committee for Clinical Laboratory Standards, Performance Antimicrobial Susceptibility of Flavobacteria, 41, 1997.
[34] National Committee for Clinical Laboratory Standards, Reference Method for Broth Dilution Antifungal Susceptibility Testing of Conidium-Forming Filamentous Fungi: Proposed Standard M38-A, NCCLS, Wayne, PA, USA, 2002.
[35] National Committee for Clinical Laboratory Standards, Method for Anlifungal Disk Diffusion Susceptibility Testing of Yeast: Proposed Guideline M44-P, NCCLS, Wayne, PA, USA, 2003.
[36] National Committee for Clinical Laboratory Standards, Methods for dilution antimicrobial susceptibility tests for bacteria that grow aerobically. Approved standard M7–A3, National Committee for Clinical Laboratory Standards, Villanova, PA. 1993.
[37] P. Skehan, R. Storeng, J. Nat. Cancer Inst. 82 (1990) 1107.
[38] J. Geary, Coord. Chem. Rev. 7 (1971) 81.
[39] C.D. Sheela, C. Anitha, P. Tharmaraj, D. Kodimunthri, J. Coord. Chem. 63 (2010) 884.
[40] H.T. Chifotides, K.R. Dunbar, N. Katsaros, G. Pneumatikakis, J. Inorg. Biochem. 55 (1994) 203.
[41] V. Shrivastava, S.K. Shrivastava, A.P. Mishra, J. Indian Chem. Soc. 22 (1995) 434.
[42] C.M. Sharaby, Spectrochim. Acta 62 A (2005) 326.
[43] S.A. Abdel-Latif, H.B. Hassib, Y.M. Issa, Spectrochim. Acta A 67 (2007) 950.
[44] M.N. Patel, P.A. Dosi, B.S. Bhatt, Appl. Organometal. Chem. 25 (2011) 653.
[45] M.H.W. Lam, Y.Y. Tang, K.M. Fung, X.Z. You, W.T. Wong, Chem. Commun. 21 (1997) 957.
[46] M.S. Masoud, F.A. Mohamed, A.M. Ramadan, G.M. El-Ashry, Spectrochim. Acta A 69 (2008) 230.
[47] Y. Song, I.A. Koval, P. Gamez, G.A. van Albada, I. Mutikainen, U. Turpeinen, J. Reedijk, Polyhedron 23 (2004) 1769.
[48] A.B.P. Lever, Inorganic Electronic Spectroscopy, second ed., Elsevier Science Publishers, Netherlands, 1984.
[49] B.N. Bessy Raj, M.R. Prathapachandra Kurup, E. Suresh, Spectrochim. Acta A 71 (2008) 1253.
[50] M.T. Tarafder, A. Kasbollah, K.A. Crouse, A.M. Ali, B.M. Yamin, H.K. Fun, Polyhedron 20 (2001) 2363.
[51] J. Ribas, C. Diaz, R. Costa, Y. Journaux, C. Mathoniere, O. Kahn, A. Gleizes, Inorg. Chem. 29 (1990) 2042.
[52] S. Basak, S. Sen, S. Mitra, C. Marschner, W.S. Sheldrick, Struct. Chem. 19 (2008) 115.
[53] T. Rosu, E. Pahontub, C. Maxima, R. Georgescuc, N. Stanicad, A. Guleae, Polyhedron 30 (2011) 154 (and references therein).
[54] A.S. El-Tabl, J. Chem. Res. 1 (1981) 19.
[55] D. Kivelson, R. Neeman, J. Chem. Phys. 35 (1961) 149.
[56] A. Syamal, Chem. Edu. 62 (1985) 143.
[57] K.K. Narang, V.P. Singh, Trans. Met. Chem. 21 (1996) 507.
[58] M.F. El- Shazly, L.S. Retaat, Trans. Met. Chem. 6 (1981) 10.
[59] A.S. El-Tabl, Trans. Met. Chem. 23 (1998) 63.
[60] R.M. Issa, S.A. Azim, A.M. Khedr, D.F. Draz, J. Coord. Chem. 62 (2009) 1859.
[61] S. Basak, S. Sen, S. Mitra, C. Marschner, W.S. Sheldrick, Struct. Chem. 19 (2008) 115.
[62] Z.D. Matovic, B. Ristic, M. Joksovic, S.R. Trifunovic, Trans. Met. Chem. 25 (2000) 720.
[63] F.H. Allen, O. Kennard, D.G. Watson, L. Brammer, A.G. Open, R. Taylor, J. Chem. Soc. Perkin Trans. 2 (1987) S1.
[64] S.J. Lippard, J.M. Berg, Principles of Bioorganic Chemistry, University Science Book, Mill Valley, 1994.
[65] Z.H. Chohan, Appl. Organomet. Chem. 20 (2006) 112.
[66] W.T. Shier, Mammalian Cell Culture on $5 a Day: A Lab Manual of Low Cost Methods, University of the Philippines, Los Banos, 1991.